JOURNAL OF GEOPHYSICAL RESEARCH, VOL. 113, D07103, doi:10.1029/2007JD009087, 2008

Incorporating water table dynamics in climate modeling: 3. Simulated groundwater influence on coupled land-atmosphere variability

Richard O. Anyah,[1] Christopher P. Weaver,[1,2] Gonzalo Miguez-Macho,[3] Ying Fan,[4] and Alan Robock[1]

Received 20 June 2007; revised 21 October 2007; accepted 30 November 2007; published 4 April 2008.

[1] Using a coupled regional climate-hydrologic modeling system, RAMS-Hydro, we investigate the role of the water table dynamics in controlling soil moisture, evapotranspiration (ET), boundary layer dynamics, and precipitation. In an earlier study we showed that a shallow water table can primarily exist in two types of hydrologic settings in North America: the humid river valleys and coastal regions in the east and the arid or semiarid intermountain valleys in the west. We also showed that the shallow water table in these settings can lead to significantly wetter soils than would exist without the presence of the water table. Here, we show that the water table−induced wetter soil directly maps into enhanced ET in the western setting, where soil water is a strong limiting factor of ET flux, but it is less likely to be the case in the more humid eastern setting where soil water is not limiting in general. We also ask whether any resulting enhanced ET will directly map into enhanced precipitation. Our hypothesis is that this can occur through two primary mechanisms: local, ET-driven enhancement of convective precipitation and enhanced regional or lateral moisture convergence caused by altered soil moisture fields, and hence altered ET, far from the region of concern. We find that, indeed, water table−induced higher ET in the arid west results in greater convective precipitation and that ET-precipitation coupling is primarily through local feedback pathways and precipitation recycling, with the main role of large-scale moisture convergence as an initiator of convection following dry periods. Transitioning to the more humid regions farther east, the greater atmospheric (relative to surface) control of precipitation progressively obscures any potential effects of the water table, and the effects of large-scale moisture convergence tend to dominate.

Citation: Anyah, R. O., C. P. Weaver, G. Miguez-Macho, Y. Fan, and A. Robock (2008), Incorporating water table dynamics in climate modeling: 3. Simulated groundwater influence on coupled land-atmosphere variability, *J. Geophys. Res.*, *113*, D07103, doi:10.1029/2007JD009087.

1. Introduction

[2] This paper concludes a three-part series aimed at investigating the influence of water table dynamics in the warm season coupled land-atmosphere system. In part 1, *Fan et al.* [2007] examined the spatial and temporal structure of the observed water table depth in the lower 48 states of the U.S. and constructed an equilibrium water table over North America constrained by these observations. They found that water table depth exhibits spatial organization at regional and continental scales. Shallow water table conditions occur primarily in two types of environments. The first is in a humid climate with flat terrain, such as in the river valleys and coastal regions of the eastern U.S., where the abundant vertical flux, combined with the slow surface and subsurface drainage, leads to a shallow water table. The second is in arid or semiarid climates with large-scale topographic relief, such as in the intermountain valleys of the western U.S., where snow in the mountains feed the aquifers in the valleys through river and groundwater convergence, causing the water table to rise near the land surface despite the dry climate. We suggested that it is in these two types of environments that the water table dynamics may have the strongest effect on soil moisture. In addition, time series analyses indicated that the water table exhibits diurnal, event, seasonal, and interannual variability, leading to the hypothesis that the temporal organization of soil moisture might occur at similar scales, and that the

[1]Department of Environmental Sciences, Rutgers University, New Brunswick, New Jersey, USA.
[2]Now at Global Change Research Program, U.S. Environmental Protection Agency, Washington, D. C., USA.
[3]Nonlinear Physics Group, Universidade de Santiago de Compostela, Santiago de Compostela, Spain.
[4]Department of Earth and Planetary Sciences, Rutgers University, New Brunswick, New Jersey, USA.

0148-0227/08/2007JD009087$09.00

presence of a shallow water table might influence soil moisture memory.

[3] To test these hypotheses, *Miguez-Macho et al.* [2007], in part 2, incorporated groundwater processes, with dynamic links to soil water and river flow, into the standard land surface scheme in RAMS (Regional Atmospheric Modeling System), creating RAMS-Hydro. They carried out offline simulations over North America for the 1997 warm season with prescribed atmospheric forcing. They illustrated the role of the water table in controlling soil moisture by comparing results from two runs, one with an explicitly simulated water table, and the other with free, gravity drainage at the base of the soil column. They found that wherever the water table is shallow (within capillary reach), the near-surface and root zone soil moisture was significantly higher in the run with full hydrology. This was due to the slower vertical drainage with the water table as the lower boundary of the soil, the upward capillary flux from the water table as a source for dry-period evapotranspiration (ET), and, in the intermountain valleys, the presence of lateral groundwater convergence. As hypothesized in part 1, the difference between the simulations with and without the water table was greatest in the two kinds of settings where the climatic and geologic balance yields a water table that is shallow. The simulated soil moisture was significantly higher in the humid river valleys and coastal regions of the east, and in the otherwise arid intermountain valleys of the west. They also found that the slow changing nature of the water table stabilized the temporal fluctuations in soil moisture, resulting in stronger seasonal persistence.

[4] These findings may have implications for studies of land-atmosphere interactions. It is well understood that, in certain regions and time periods, soil moisture can be a critical control on land-atmosphere fluxes, boundary layer structure, and convective precipitation [e.g., *Betts*, 2004]. The soil moisture reservoir can influence surface water and energy balance, and the persistence of soil moisture anomalies can lead to variations in the regional intensity of the water cycle, such as droughts and floods [e.g., *Entekhabi et al.*, 1996; *Timbal et al.*, 2002; *Montaldo and Albertson*, 2003; *Schubert et al.*, 2004]. This influence can be via an impact on local ET [*Pielke*, 2001; *Betts*, 2004; *Sarith and Koster*, 2005], which affects the surface energy budget, planetary boundary layer, and the convective potential energy available in the atmospheric column, hence potentially driving changes in precipitation.

[5] There are a number of confounding factors, however, that limit the ability of soil moisture anomalies to drive changes in ET, and, even more so, changes in precipitation. For example, ET is not just a function of soil moisture, but also net surface radiation, humidity, and winds, as well as factors such as the nonlinear dependence of stomatal resistance on water availability. Similarly, precipitation is not just a function of local ET, but also large-scale moisture convergence. Concepts such as "precipitation recycling ratio" [e.g., *Brubaker et al.*, 1993] reflect some of these complex interactions. In practice, therefore, the influence of local soil moisture changes on precipitation has been found to be largely limited to certain regions and seasons, in particular arid and semiarid and transitional regimes dominated by convective precipitation [*Findell and Eltahir*, 2003a, 2003b, 2003c; *Koster et al.*, 2004; *Dirmeyer*, 2006]. This is not to say that the relationship between soil moisture and precipitation is local only; it has also been shown that large-scale spatial variability in soil moisture can influence atmospheric circulation, thereby changing horizontal advection and hence water vapor convergence [e.g., *Small*, 2001; *Pal and Eltahir*, 2002; *Georgescu et al.*, 2003; *Kanamitsu and Mo*, 2003]. Thus the water table–induced spatial variability in soil moisture may influence local (vertical interaction) as well as regional (lateral interaction) atmospheric water budgets and climate dynamics.

[6] Within this context, we ask the following questions: First, to what extent will differences in simulated soil moisture, as documented in part 2, be reflected in the distribution of ET? That is, do the two regions of large soil moisture difference, humid climate plus flat terrain and arid climate plus regional hydrologic convergence, translate into regions of large ET difference? Our hypothesis is that while the water table–induced wet soil may lead to higher ET in the water-limited arid west, it will likely not affect ET much in the humid east where soil moisture is not a limiting factor. Second, if the above hypothesis is true, then does the high ET in the water-limited arid west result in a detectable difference in local precipitation? If so, what are the relative roles of local ET and large-scale moisture convergence in controlling observed differences in precipitation? We attempt to answer these questions here by using the fully coupled version of the RAMS-Hydro modeling system that was described in detail in part 2. Only offline simulations were carried out for the analyses in part 2, but here we activate the coupling between the land and atmospheric components of the model. As in part 2, we performed two parallel sets of runs, one with full horizontal and vertical water table dynamics, and the other with simple, free, gravity drainage of soil water.

2. Model Description and Experimental Design

[7] The atmospheric part of RAMS-Hydro is standard RAMS v4.3 [*Walko and Tremback*, 2000]. RAMS is a nonhydrostatic model and solves the full nonlinear equations of motion for the atmosphere on a σ_z terrain-following vertical coordinate system. The horizontal grid uses an oblique (or rotated) polar stereographic projection, where the pole is rotated to an area in the center of the simulation domain to minimize the projection's distortion in the main area of interest. An Arakawa-C grid configuration is used, with the velocity components of u, v and w defined at locations staggered one-half grid length in x, y and z directions, respectively, from the thermodynamic, moisture and pressure variables [*Arakawa and Lamb*, 1977]. It uses multiple parameterization options for subgrid-scale transport, radiation, cumulus convection and land surface processes. In the present study the parameterizations used include the Kain-Fritsch convection scheme [*Kain and Fritsch*, 1993], Harrington radiation scheme [*Harrington*, 1997] and the two-and-a-half-order Mellor and Yamada turbulence scheme [*Mellor and Yamada*, 1982]. The version of the model that we use here includes spectral nudging [*Miguez-Macho et al.*, 2004], which adds terms to the equations of motion that relax certain scales of the model solution in the domain to the same scales of the driving fields. We nudge wavelengths of about 2500 km and longer

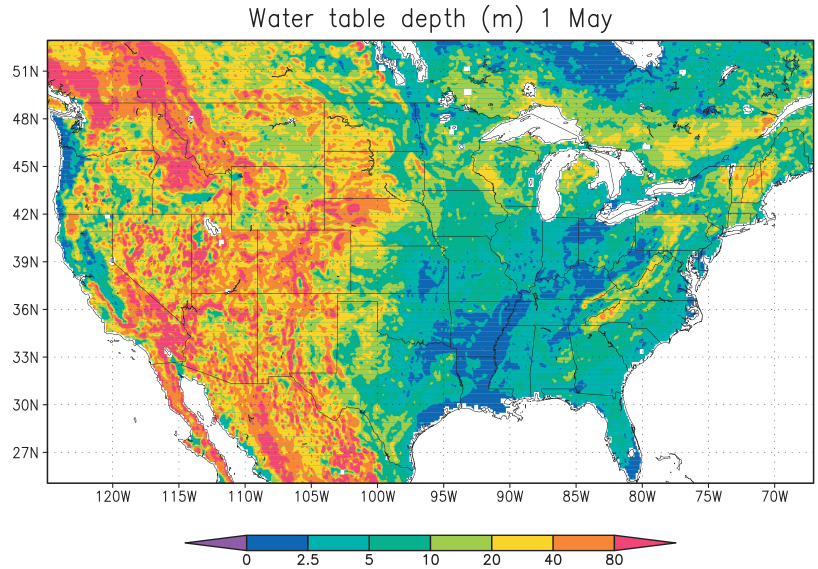

Figure 1. Water table depth (m from the surface) at the beginning of the simulation period.

in all fields but moisture, and only above the boundary layer [*Miguez-Macho et al.*, 2004, 2005]. Keeping the large scales close to those of the reanalysis avoids the unphysical distortion of the large-scale flow caused by incompatibilities of the model solution with the lateral boundary conditions, a well-known problem in regional climate simulations as documented by *Miguez-Macho et al.* [2004]. With the spectral nudging technique the large-scale flow closely follows reanalysis, thus preventing some of the feedback of the small scales onto the large scales. This is not a serious limitation, however, since, in our view, limited area models are not meant to modify the large-scale flow significantly (hence the term "dynamical downscaling"). Nevertheless, we do not nudge moisture fields, and therefore water is conserved.

[8] The land surface component in RAMS-Hydro has been fully described by *Miguez-Macho et al.* [2007]. Key changes over the standard land surface scheme include a groundwater reservoir that responds to soil water flux and lateral groundwater flow, dynamic water table–river exchange driven by elevation difference between the two reservoirs, and river flow routing to the ocean with a simple variable velocity scheme.

[9] All simulations were performed on a 50-km horizontal grid for the atmosphere, 12.5 km for land, and the model integrated on 39 unevenly spaced vertical levels. The initial and lateral boundary conditions were derived from the NCEP Reanalysis II data set [*Kanamitsu et al.*, 2002], and weekly *Reynolds et al.* [2002] sea surface temperatures were used as lower boundary conditions over the ocean portion of the computational domain. The domain covers most of North America as in the work by *Miguez-Macho et al.* [2005]. The water table–river link was spun up with a 10-year simulation, and the water table–soil moisture link was spun up with a 4-month simulation. Figure 1 shows the water table depth at the end of this process. For details see *Miguez-Macho et al.* [2007]. We performed two sets of experiments, one with the water table (hereafter referred to as WT), and the other with free drainage at the bottom of the 4-m deep soil column (hereafter referred to as FD). Both of these simulations were initialized with the same soil moisture field, as produced by the dual spin-up procedure. The simulations were performed for 6 months over the 1997 warm season (May–October). Each set is a four-member ensemble, generated by lagged initial conditions [*Hoffman and Kalnay*, 1983] on 1, 2, 3, and 5 May, respectively.

3. Comparison Between Simulated and Observed Precipitation

[10] We compare the simulated monthly precipitation over the entire U.S. between the WT and FD ensemble means, and between these simulated precipitation fields and daily, gridded rain gauge observations, for July through September (Figure 2). We treat the first 2 months (May and June) as spin up and therefore exclude this period from our analysis. For all 3 months, the spatial distribution of simulated monthly total precipitation in both FD and WT qualitatively agrees with observations in a gross sense, but with significant regional biases. For example, both simulation ensembles underestimate precipitation amounts over the Gulf Coast, much of the southern and central Great Plains, and parts of the west. One feature, most pronounced in the simulations for July (Figures 2b and 2c) and September (Figures 2g and 2h), is the drier corridor running from the Gulf Coast up to the Midwest states, approximately colocated with the position of the low-level jet. The simulated low-level jet is much stronger in the RAMS-Hydro runs than observed (not shown), so it is possible that moisture from the Gulf of Mexico is being transported farther north in the model, thus depriving the southern parts of the necessary moisture that would otherwise enhance precipitation there.

[11] From this continental-scale, monthly mean perspective, the WT and FD precipitation patterns are fairly similar to each other. In general, slightly more precipitation is simulated in WT than FD, with the largest differences (>50% in some cases) tending to occur over the arid and semiarid (water-limited) regions in the western parts of the

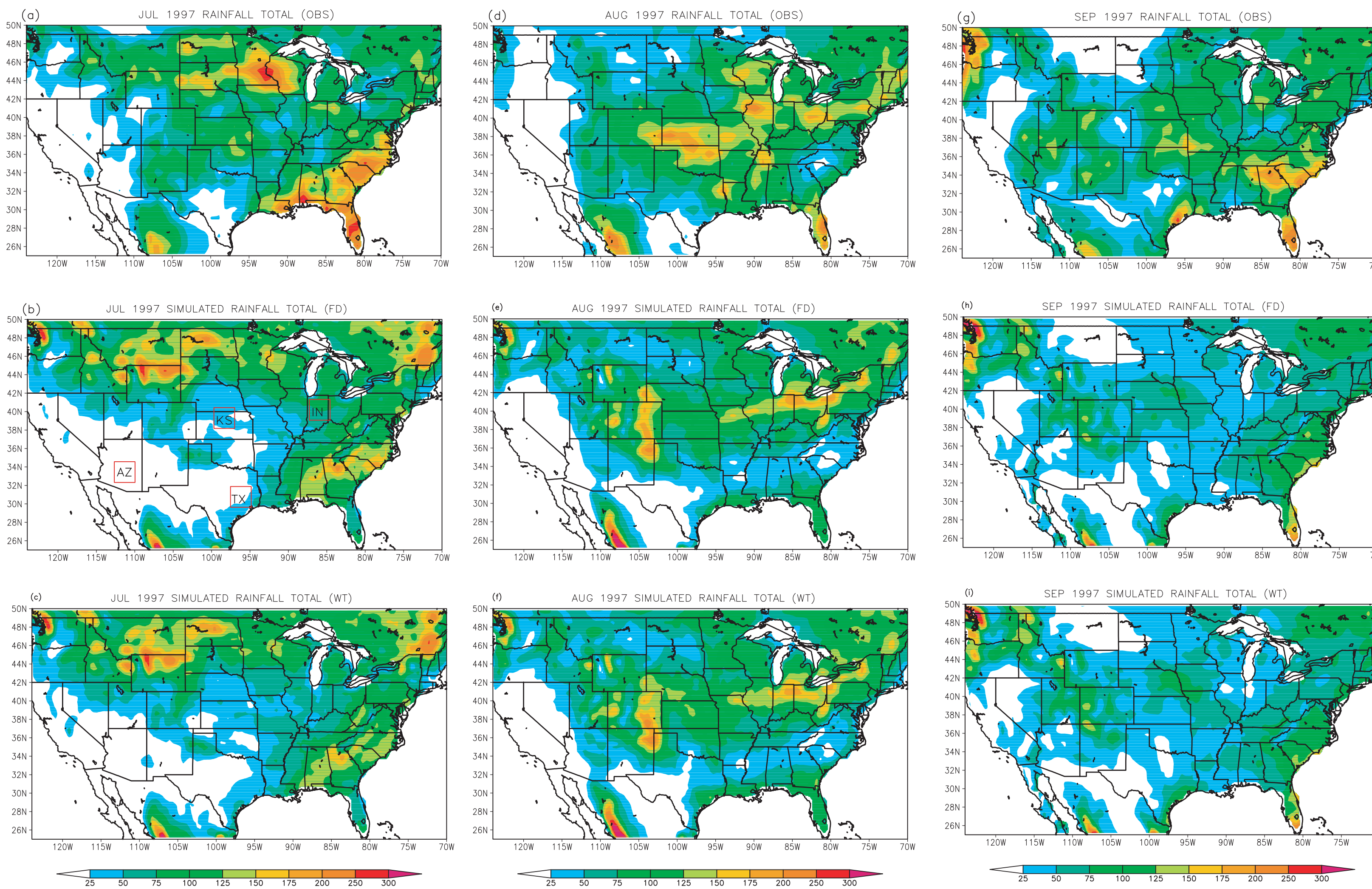

Figure 2. Monthly rainfall total (mm) for (a–c) July, (d–f) August, and (g–i) September, showing observations (Figures 2a, 2d, and 2g), free drain (FD) simulations (Figure 2b, 2e, and 2h), and water table (WT) simulations (Figures 2c, 2f, and 2i). Figure 2b shows four boxes for regions analyzed further. Arizona (AZ) and southern Texas (TX) are in arid, water-limited, environments, while the other two, Kansas (KA) and Indiana (IN), are located in relatively humid climates, and evapotranspiration is more energy-limited.

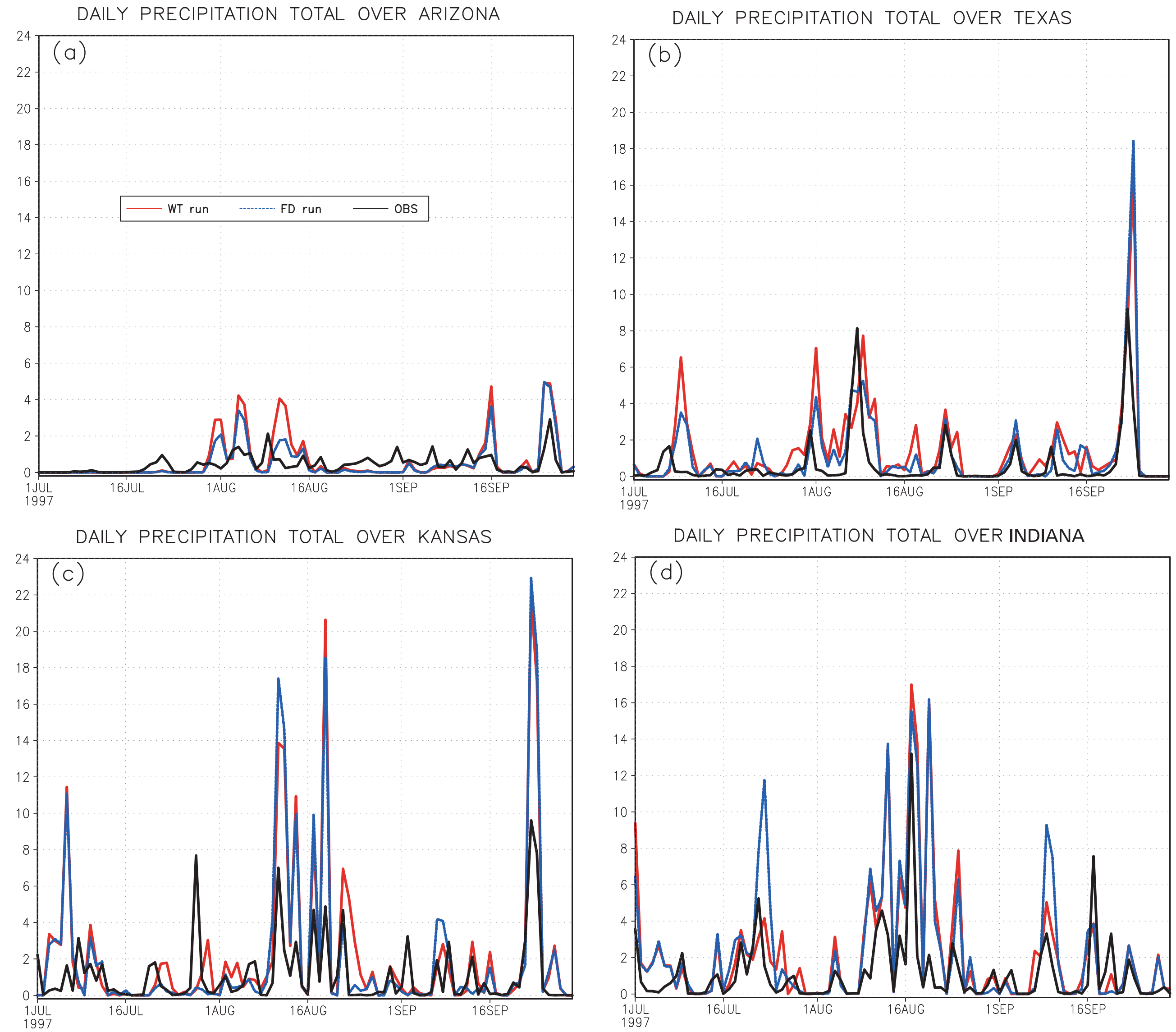

Figure 3. Daily time series of precipitation (mm) for the ensemble mean of WT (red) and FD (blue), compared to observations (black), over the four boxes shown in Figure 2b, (a) Arizona, (b) Texas, (c) Kansas, and (d) Indiana.

domain (e.g., southern California, Arizona, southern Texas, and the southern plains), though with significant regional variability. We focus on these precipitation differences between the two ensembles more closely throughout the rest of the paper, especially from a regional and event-scale perspective (as opposed to the continental and monthly perspective of Figure 2). One important note is that the differences in the WT and FD results shown here are likely not as large as they could be with a different experimental design. This is because, as noted previously, both sets of simulations were initialized with the same soil moisture field, produced via a comprehensive spin-up that included the full effects of the dynamic water table. Because of the strong persistence of soil moisture over timescales of months, even the FD simulations thus include to some degree the "benefits" of the enhanced hydrology of the WT runs. In addition, our soil column is 4 m deep, which has a substantial storage and hence a slow response to the disabling of the water table component.

[12] Figure 3 shows the simulated daily precipitation total for July through September, averaged over four regional boxes, along with the observed values. Locations of the four boxes are shown in Figure 2. The Arizona (AZ) box is located in an arid, water-limited environment, the Indiana (IN) box is located in a humid, energy-limited environment, and the Texas (TX) and Kansas (KS) boxes are located in transition regions between the two. Overall, both the WT and FD ensembles roughly capture the frequency, timing, and magnitude of the individual observed precipitation events.

[13] It is important to emphasize that our aim in this paper is not to demonstrate that including a dynamic water table improves the simulation of, for example, the continental-scale spatial patterns of monthly mean precipitation compared to observations. As discussed in the Introduction,

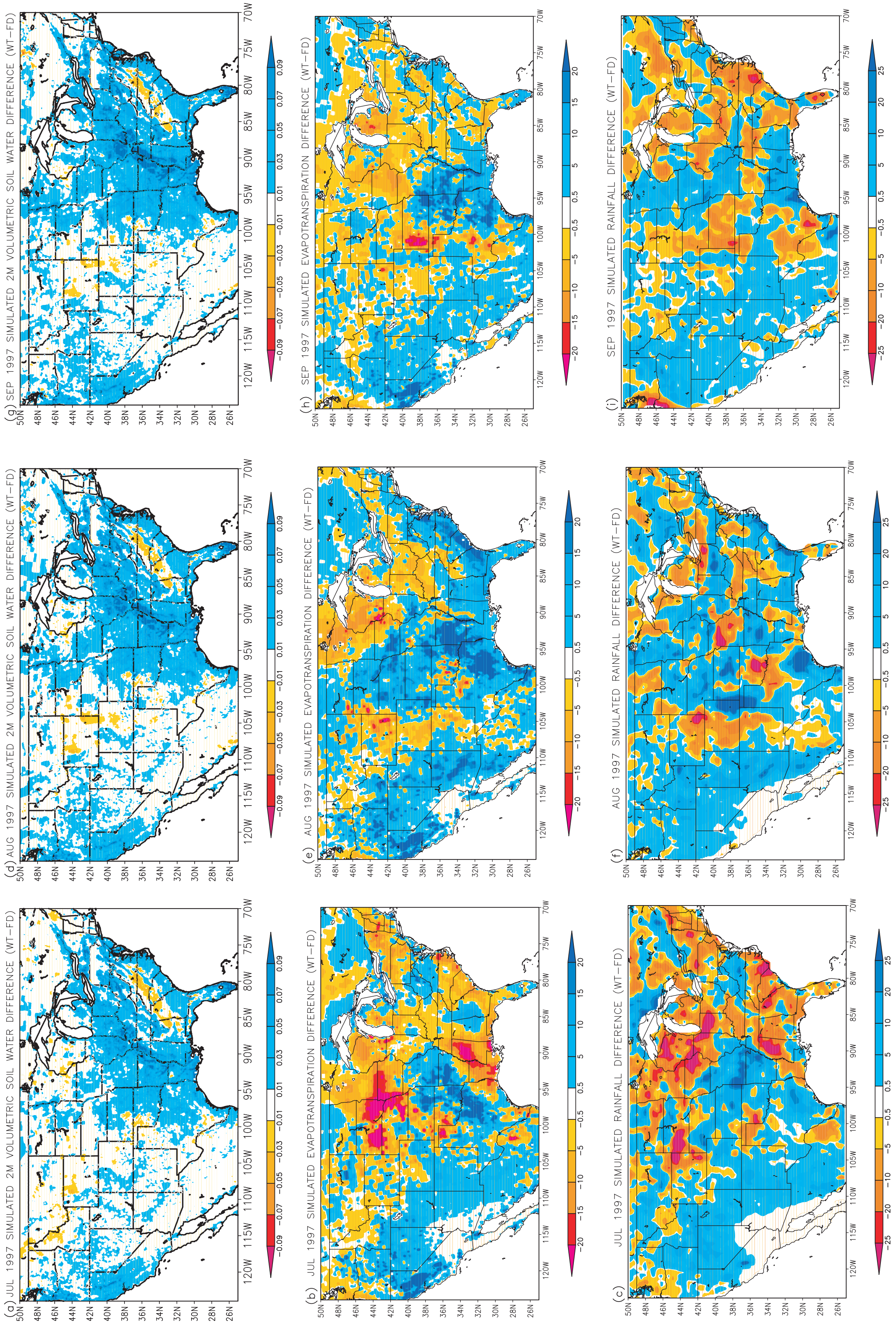

Figure 4. (a–c) July, (d–f) August, and (g–i) September differences in monthly root zone (top 2 m) soil moisture ($m^3\ m^{-3}$) (Figures 4a, 4d, and 4g), evapotranspiration (mm) (Figures 4b, 4e, and 4h), and precipitation (mm) (Figures 4c, 4f, and 4i).

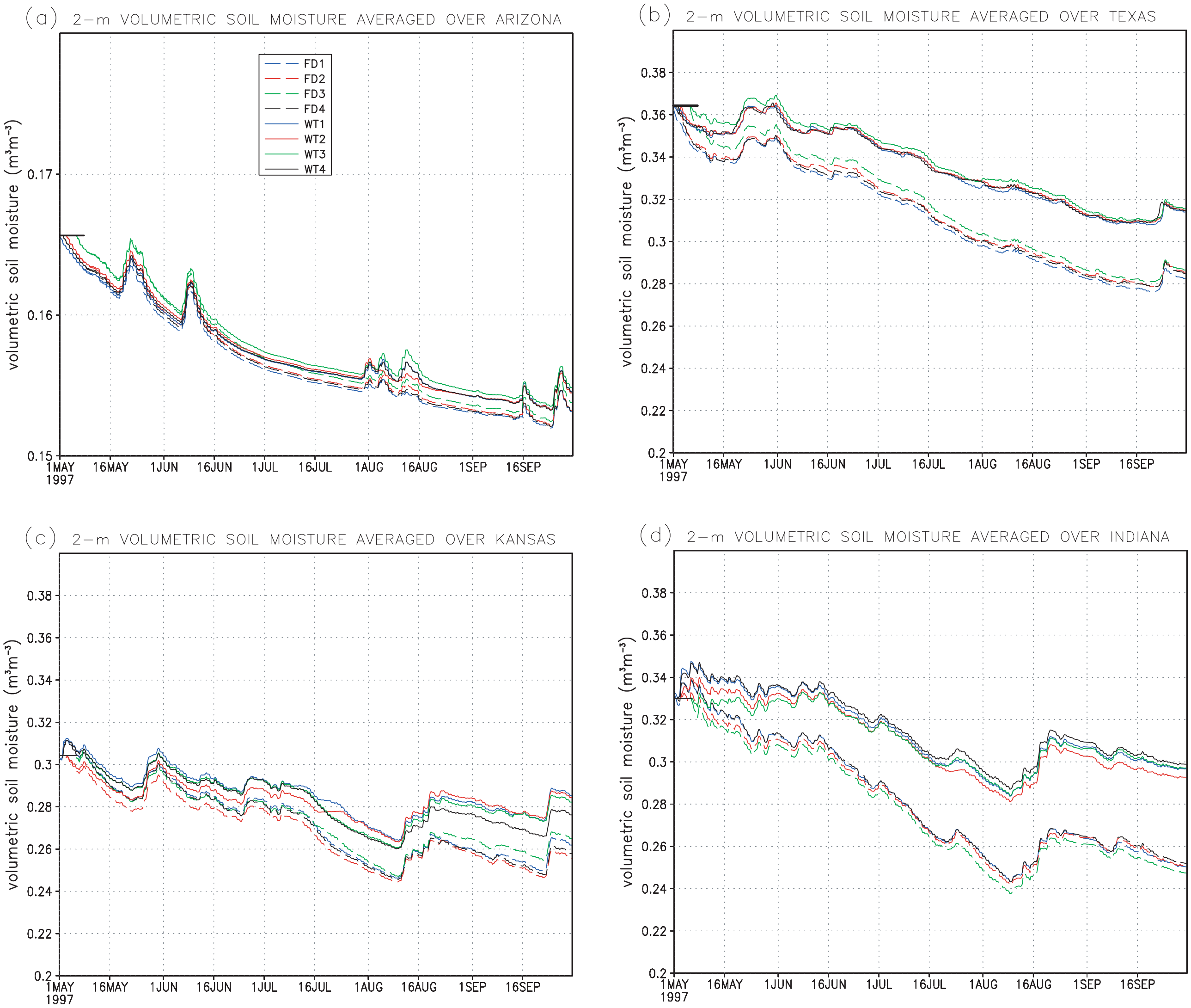

Figure 5. WT and FD ensemble simulations of the root zone volumetric soil moisture averaged over four regional boxes (a) Arizona, (b) Texas, (c) Kansas, and (d) Indiana. Locations of the boxes are given in Figure 2b. The vertical scale for Figure 5a is twice that of the other panels, so the small variations can be more easily seen.

numerous factors confound the potential influence of land surface conditions on precipitation. At this stage, our goal is simply to examine the role that the water table plays in the pathways that couple land hydrology with atmospheric processes, in the context of these confounding factors. In addition, other sources of bias that are separate from the representation of land surface processes, e.g., parameterization deficiencies and errors in the simulated circulation patterns (see above), make it difficult to quantitatively evaluate the full extent of any performance gains that might be associated with including groundwater dynamics. Finally, the impact of the soil moisture initialization on the results, as discussed above, also has implications for evaluating the relative performance of the WT model configuration. Our hope is that improved basic understanding of the coupled groundwater-soil moisture-atmospheric system arising from the sensitivity analysis in this paper will provide the basis for more targeted investigations of possible benefits for improving simulated precipitation.

[14] Now we examine in more detail the differences between the two sets of simulations and attempt to answer the questions posed in the Introduction.

4. From Soil Moisture to ET and From ET to Precipitation

4.1. Spatial Patterns

[15] To illuminate possible regions in which the spatial patterns introduced into the land surface by incorporating the water table are conveyed to the atmosphere, and vice versa, we show in Figure 4 the WT-FD difference in root zone volumetric soil water, ET, and precipitation for July through September. Consistent with the results of *Miguez-Macho et al.* [2007], where comparisons were made between offline WT and FD simulations, Figure 4 shows large soil moisture differences in locations with shallow water tables, such as the humid river valleys and coastal regions of the east and the intermountain valleys of the

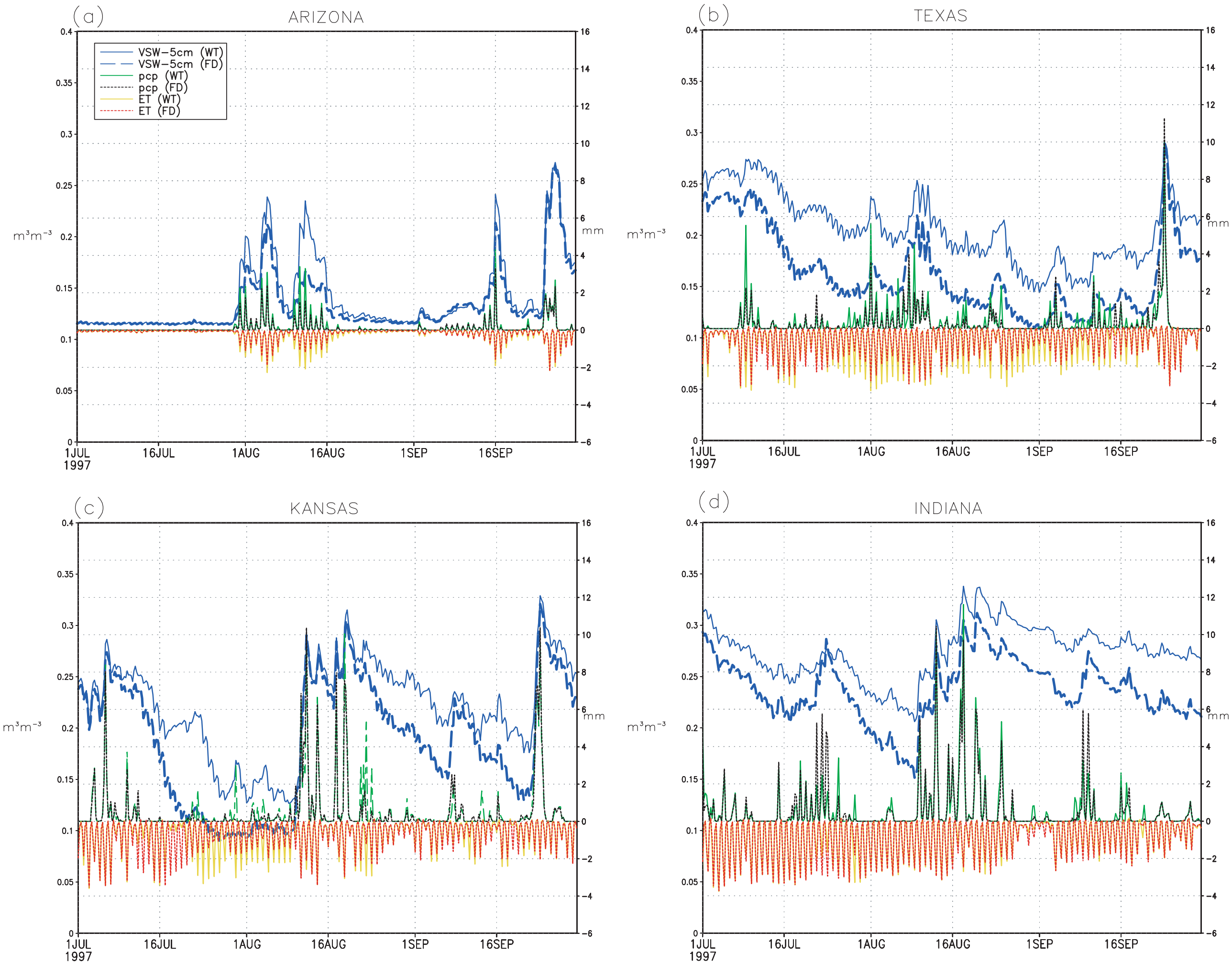

Figure 6. Daily time series of top-5-cm soil moisture (m^3 m^{-3}, VSM-5cm), evapotranspiration (mm, ET), and precipitation (mm, pcp), with ET values inverted. The soil moisture values over Arizona are doubled to fit the same scale used in the other three regions.

west. The water table depth pattern does not change significantly from the initial conditions shown in Figure 1 over the simulation period, as in the off-line simulations from *Miguez-Macho et al.* [2007].

[16] The wetter soil is directly translated, and in some places magnified (e.g., in August in Arizona and Nevada), into higher ET, in the arid regions of the west and the southern Great Plains, in all 3 months. In the eastern half of the domain, particularly in the Great Lakes states, the wetter soil actually leads to lower ET in all 3 months. The soil moisture-ET link can be relatively straightforward in arid regions where the sky is clear and the soil water is the limiting factor, but the relationship is typically much more complex in a humid climate where the sky is often cloudy and surface energy is the limiting factor.

[17] Going further up the chain of linkages, we note that the higher ET in the western states seems to correspond to higher precipitation, but the relationship in the eastern states is again obscured. The latter relationship provides a glimpse of the complexity of the interplay between water and energy, and the vertical and the lateral atmospheric fluxes in controlling precipitation.

4.2. Temporal Patterns

[18] The primary coupling between ET and precipitation occurs over event to synoptic scales. Therefore, we examine time series of land and atmospheric quantities to better understand the interplay between soil water processes, ET, and precipitation over these timescales.

[19] Figure 5 shows the daily time series of root zone (top-2-m) volumetric soil moisture from May, when the two drainage schemes are applied, through September, for the individual WT and FD ensemble members. The soil moisture is spatially averaged over the four boxes described above. A few points emerge from Figure 5. First, there is a clear separation between the WT and FD runs for all four regions. Second, not only is it that the WT and FD curves slowly diverge, but also that the dynamic response of soil moisture to precipitation events differs. The WT runs tend to respond less steeply at the onset of the events, and the signal of these events tends to decay more slowly than in the FD runs. In other words, the presence of the water table seems to dampen the soil moisture variability at event to synoptic scales in these coupled land-atmosphere simula-

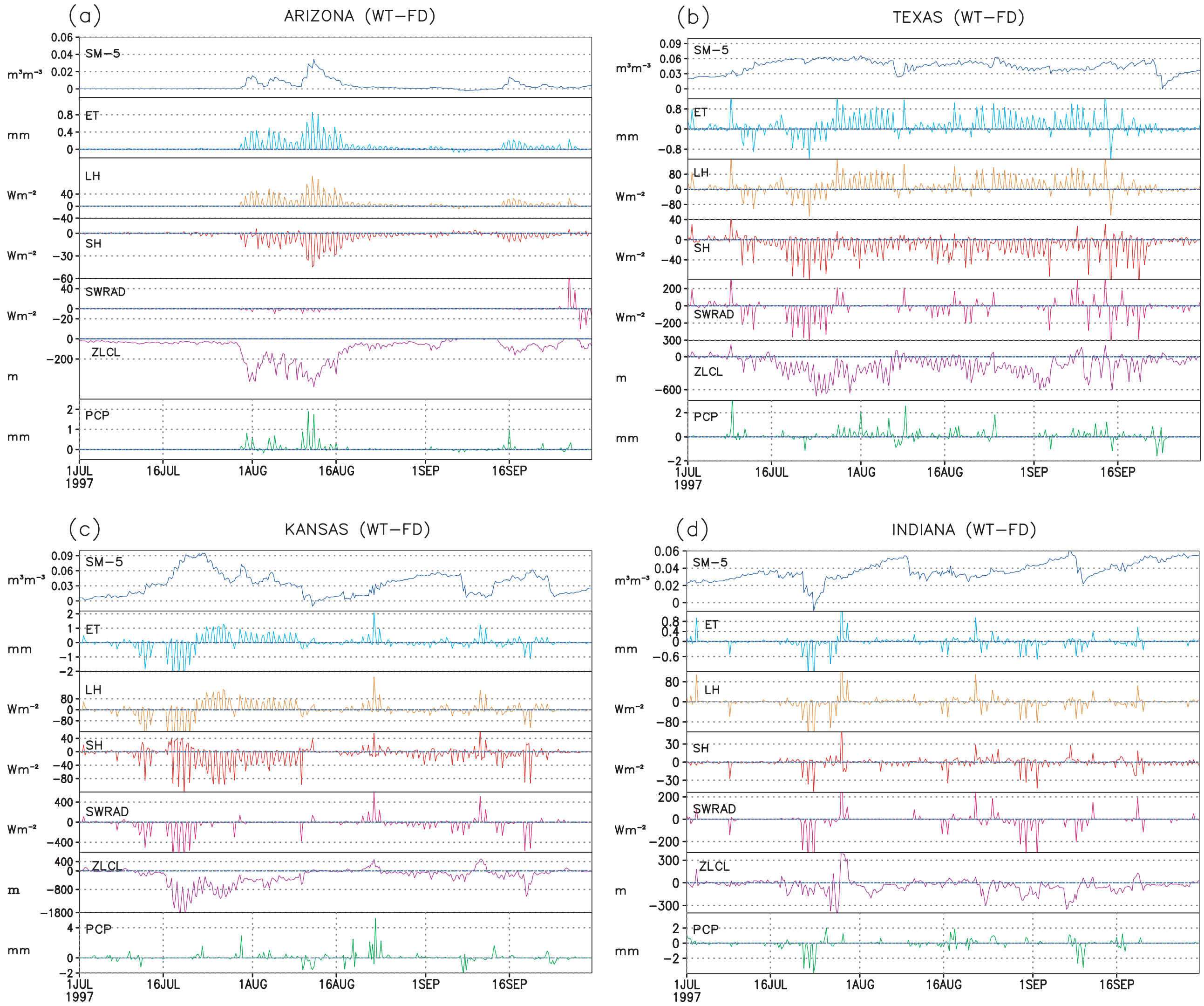

Figure 7. WT-FD differences showing diurnal evolution of top-5-cm soil water (SM-5), ET, latent heat (LH), sensible heat flux (SH), shortwave radiation (SWRAD), lifted condensation level (ZLCL), and precipitation (PCP).

tions, consistent with the offline findings of *Miguez-Macho et al.* [2007].

[20] These points are illustrated in a more detailed manner in Figure 6, which shows the 6-h WT and FD ensemble mean values of top-5-cm soil moisture, precipitation, and ET for the months of July, August, and September. Complementing these results, Figure 7 shows differences between the WT and FD ensemble means for soil moisture, ET, latent and sensible heat flux (LH and SH), surface incident shortwave radiation (SWRAD), the lifted condensation level (ZLCL) as a proxy for cloud base height, and precipitation. We show top-5-cm soil moisture here to emphasize the higher variability in the near-surface soil water that is most readily available for evaporation.

[21] Over the AZ box (Figures 6a and 7a), the strong diurnal, event, and synoptic coupling between the land and atmospheric boundary layer state is particularly evident from the plots. Soil moisture, ET, LH, and precipitation are all generally larger in the WT ensemble, while SH and ZLCL are all generally lower. The slower drainage and availability of water table–fed soil moisture in the WT ensemble sustains higher ET, which in turn influences boundary layer structure and convection. As discussed by *Fan et al.* [2007] and shown in Figure 1, while the water table is quite deep over much of AZ (>40 m), there are also numerous locations throughout the state (e.g., intermountain valleys) where the water table rises much closer to the surface. It is the contribution of these locations that produce the differences between WT and FD seen in the box averages.

[22] These results from the AZ box are consistent with the large body of work showing how moister surface conditions in water-limited environments are propagated through land-atmosphere fluxes to the atmosphere [e.g., *Betts*, 2004]. Mean SWRAD (not shown) is uniformly high in both the WT and FD ensembles there, reflecting how ET is not limited by surface energy.

[23] Over the other three boxes, the relationships are not as obvious, so additional analysis is needed to untangle the

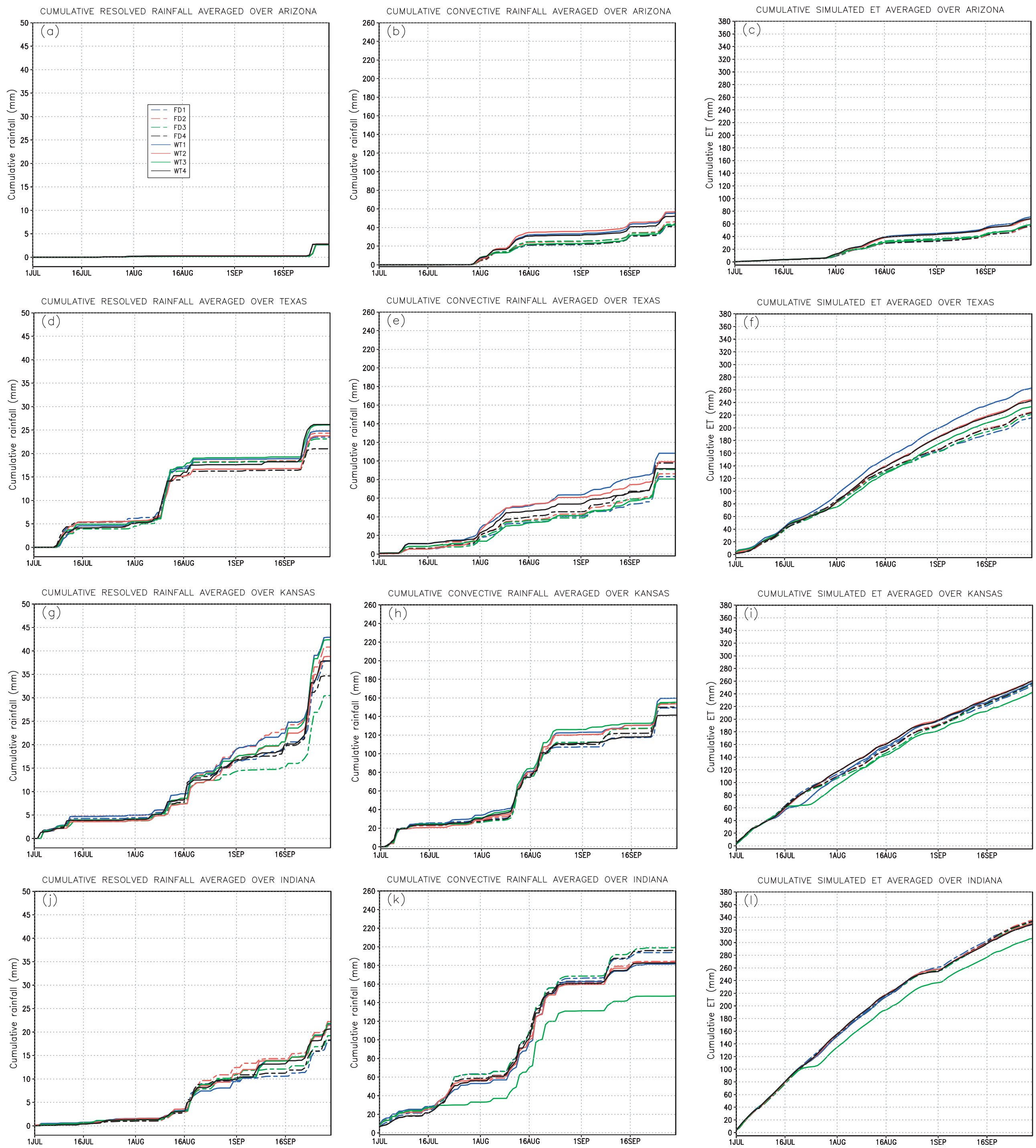

Figure 8. Cumulative values of large-scale resolved precipitation, convective precipitation, and evapotranspiration, all in mm, over the four boxes: (a–c) Arizona, (d–f) Texas, (g–i) Kansas, and (j–l) Indiana.

interactions. Specifically, in the following subsection, we analyze the water budgets of all four boxes.

[24] Before examining those results, however, we also show cumulative, area-averaged warm-season precipitation and ET for all four boxes and ensemble members (Figure 8). Here we have divided total precipitation into its resolved and convective components (as represented in RAMS-Hydro). Note the difference in vertical axis between the resolved and convective precipitation plots, which reflects the dominance of convective precipitation in all four boxes during this time period. For the AZ box (Figures 8a–8c), there is no clear distinction between the WT and FD ensemble members in the resolved component of precipitation (which is very small) but a clear separation for the convective component. In other words, AZ precipitation is largely contributed by local convection, which is also where

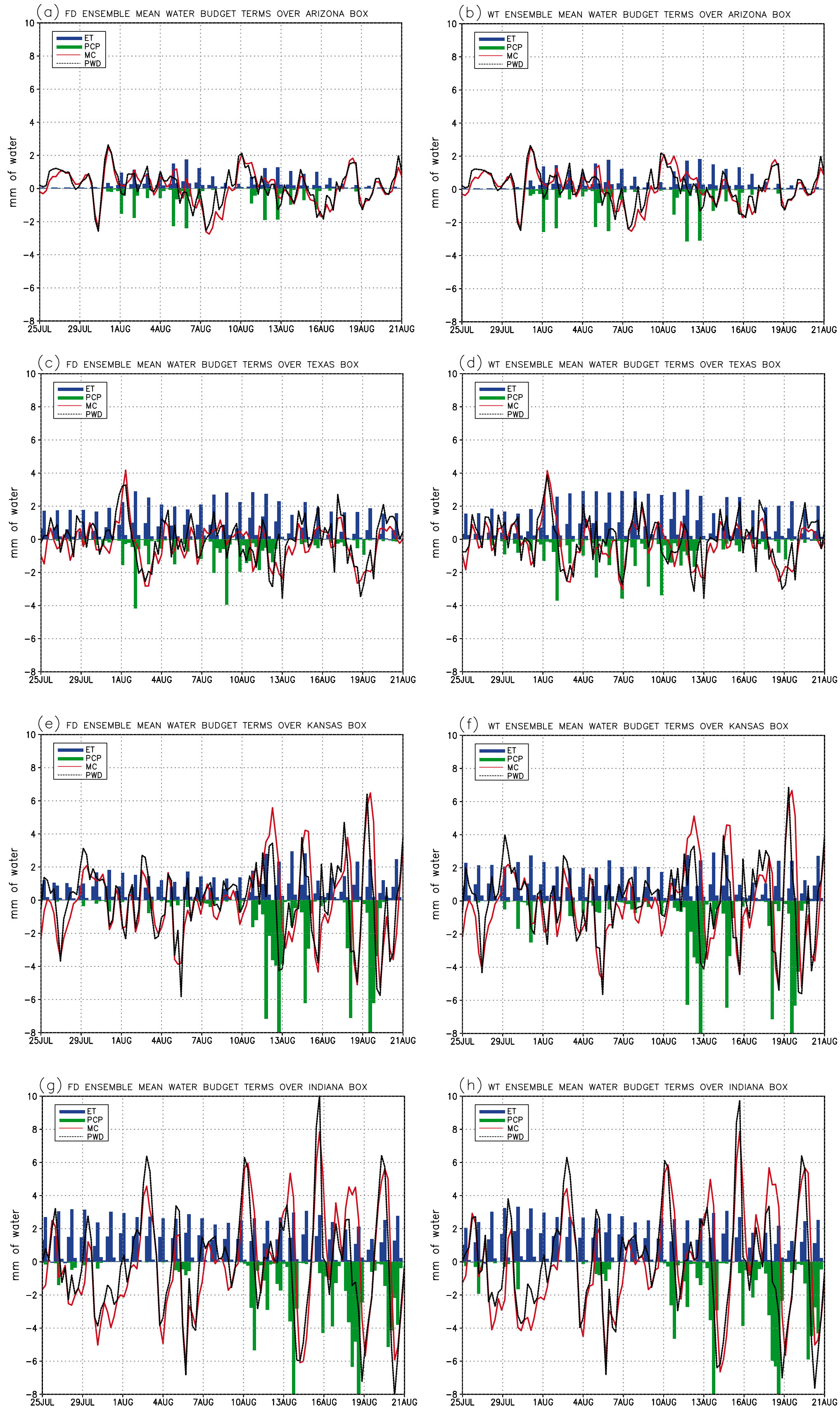

Figure 9. Time series of ensemble mean precipitation (PCP, green bar), evapotranspiration (ET, blue bar), moisture convergence (MC, red line), and precipitable water (PWD, black line) for (a and b) Arizona, (c and d) Texas, (e and f) Kansas, and (g and h) Indiana. Precipitation values are inverted.

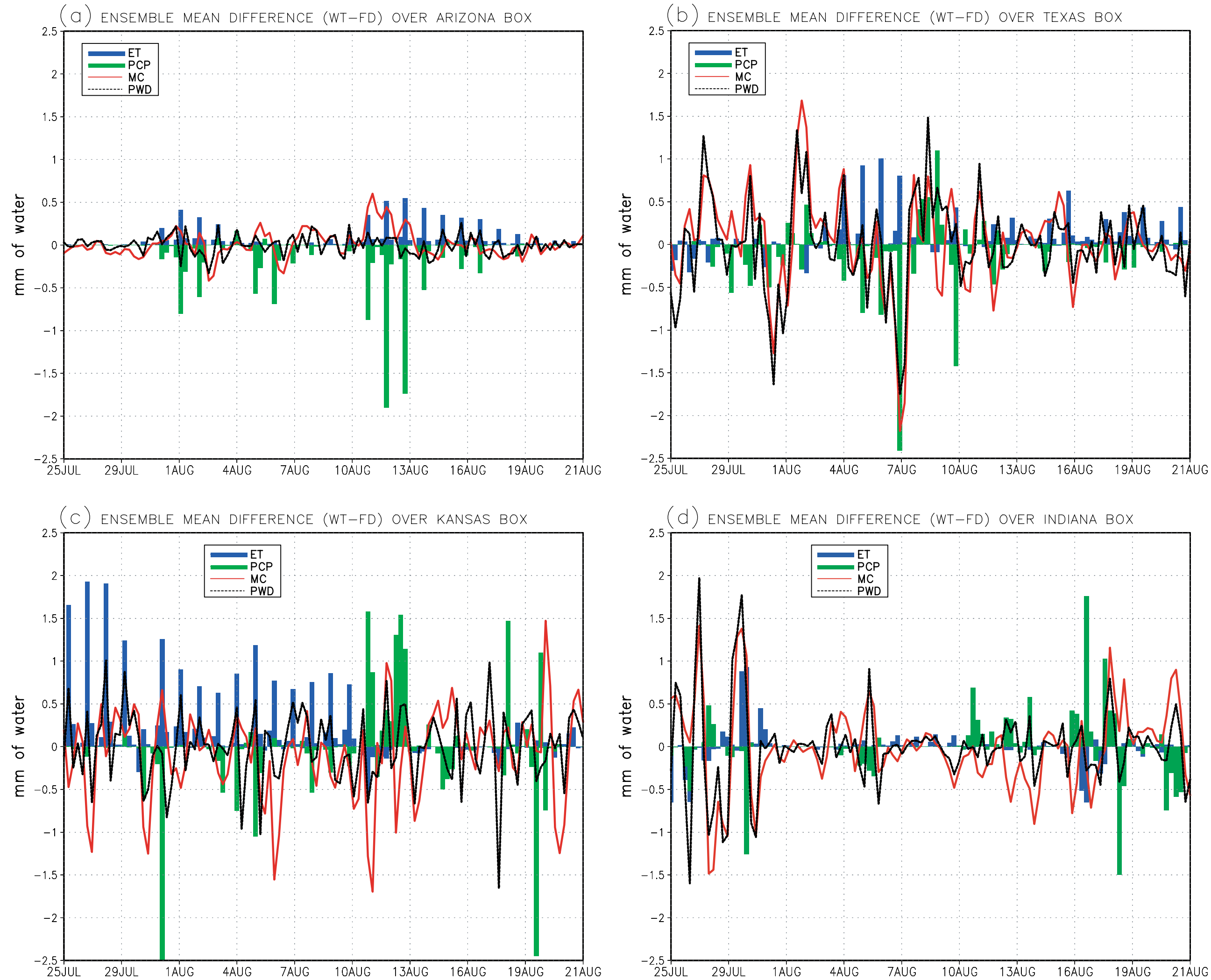

Figure 10. Time series of ensemble mean differences (WT-FD) for (PCP, green bar), evapotranspiration (ET, blue bar), moisture convergence (MC, red line), and precipitable water (PWD, black line) for (a) Arizona, (b) Texas, (c) Kansas, and (d) Indiana. Precipitation values are inverted.

the effect of the presence of the water table is felt. Furthermore, the precipitation difference between the WT and FD ensembles is comparable to the ET difference, again consistent with a strong local land-atmosphere coupling.

[25] One exception to the distinct separation between WT and FD simulations is the WT3 member, which has an accumulation comparable to the FD group. This is because it misses several rainfall events in the AZ box during the 1–6 August period (the WT3 run is also anomalous in either convective precipitation or ET, or both, in the other three boxes as well). This exception illustrates a couple of points. First, convective precipitation is inherently patchy, triggered by small-scale disturbances and areas of instability that have a significant stochastic component at the simulation scales of this study. Second, because of this high variability in convection-dominated regimes, an ensemble approach to this type of model-based sensitivity study is useful for developing more robust conclusions.

[26] Over the TX (Figures 8d–8f) and KS (Figures 8g–8i) boxes, there is a less clear distinction between the WT and FD ensembles for convective precipitation, though there is still some separation. This separation is essentially absent in the IN box (Figures 8j–8l). For resolved precipitation, the WT and FD runs are more or less mixed together for all three boxes. Finally, for ET, there is some systematic difference between the WT and FD ensembles for the TX box, less so for the KS box, and essentially no difference for the IN box, consistent with progressively weaker land-atmosphere coupling as we move from drier to wetter environments.

4.3. Water Budget Analysis

[27] To examine the links between land and atmosphere in more detail, we calculate the atmospheric water budget terms for all four boxes. We focus on the period 25 July to 21 August, when significant rainfall occurred in each box. The terms examined are ET, precipitation, horizontal moisture convergence (MC), and the change in atmospheric storage (precipitable water), all in mm/d. The latter two terms are integrated over the depth of the atmosphere.

Table 1a. Atmospheric Water Budget Terms for the Arizona and Texas Boxes (See Figure 2b) for 25 July to 21 August[a]

0000 UT 25 Jul to 1800 UT 21 Aug	WT1	WT2	WT3	WT4	WT Ensemble Mean	FD1	FD2	FD3	FD4	FD Ensemble Mean	WT − FD Ensemble Mean
					Arizona Box						
Evapotranspiration	1.308	1.268	0.968	1.264	1.200	0.912	0.932	1.052	0.928	0.956	0.244
Precipitation	1.152	1.116	0.800	1.256	1.080	0.760	0.772	0.896	0.868	0.824	0.256
Moisture convergence	0.360	0.412	0.276	0.308	0.340	0.292	0.252	0.320	0.264	0.284	0.056
Change in precipitable water	0.576	0.560	0.560	0.576	0.560	0.576	0.576	0.560	0.576	0.576	−0.016
Residual	−0.060	0.004	−0.116	−0.260	−0.100	−0.132	−0.164	−0.084	−0.252	−0.160	0.060
					Texas Box						
Evapotranspiration	3.528	3.300	2.852	3.272	3.238	2.800	2.964	2.980	2.984	2.932	0.306
Precipitation	1.936	1.692	1.356	2.036	1.755	1.348	1.540	1.556	1.412	1.464	0.291
Moisture convergence	−0.944	−0.992	−1.096	−0.528	−0.890	−1.108	−0.940	−0.888	−0.996	−0.983	0.093
Change in precipitable water	0.192	0.140	0.184	0.104	0.155	0.100	0.052	0.080	0.040	0.068	0.087
Residual	0.456	0.476	0.216	0.604	0.438	0.244	0.432	0.456	0.536	0.417	0.021

[a]Units are mm/d.

[28] Figure 9 shows time series of all the budget terms for all four boxes for the FD and WT ensemble means, separately, while Figure 10 shows the differences between the WT and FD ensemble means. (In both Figures 9 and 10 the precipitation values are inverted for visual clarity.) Tables 1a and 1b summarize the budget terms for the individual ensemble members and the ensemble means. Because we calculated horizontal moisture fluxes using the 6-h mean wind and moisture values that the model archived, rather than at each time step, there is a small residual term in the water balance, but time series (not shown) show that it is 1–2 orders of magnitude less than the instantaneous MC values, and thus not of consequence. Even for the entire time period we studied, it is much smaller than ET or precipitation (generally the largest terms in all boxes), and, for the AZ and TX boxes, tends to be significantly smaller than MC as well. The following budget discussions are based on ensemble means. As described above, the WT3 simulation is somewhat of an outlier and will tend to make any distinctions between the WT and FD ensembles somewhat more fuzzy than if it were excluded from the analysis.

[29] For the AZ box (Figures 9a and 9b), we see that, in both the WT and FD ensembles, there are dry periods punctuated with periods of rainfall events and much higher ET activity. There are two such wet periods, starting on about 31 July and 11 August, respectively. Convection seems to be initiated at the beginning of each wet period with a pulse of positive MC (enhanced convergence). Immediately after the onset of precipitation, MC hovers around zero, while ET stays large and seems to sustain additional precipitation, which in turn drives additional ET (recycling). Toward the end of each little-more-than-week-long wet period, the rain tapers off and the moisture from the last couple of days of enhanced ET is transported out of the box, as reflected in the negative MC pulse (divergence). This basic sequence plays out similarly in both the WT and FD ensembles.

[30] The difference between the simulations in this box, as already discussed, is in the amount of rainfall and ET. From Figure 10a and Tables 1a–1b, we see that both ET and P are larger in the WT compared to the FD ensemble. MC is also slightly more positive in the WT ensemble over the month, but the magnitude of the difference compared to FD is much smaller than the differences in either ET or precipitation. Therefore, to first order, the increase in precipitation in the WT ensemble can be explained by the increase in ET, with MC playing a very small role except to provide the initial water availability on synoptic timescales.

[31] In the TX and KS boxes the situation is not as straightforward, though some elements of the AZ story still hold true. In the TX box (Figures 9c and 9d), instead of two distinct wet periods as in the AZ box, there is a single, longer period of greater precipitation starting

Table 1b. Atmospheric Water Budget Terms for the Kansas and Indiana Boxes (See Figure 2b) for 25 July to 21 August[a]

0000 UT 25 Jul to 1800 UT 21 Aug	WT1	WT2	WT3	WT4	WT Ensemble Mean	FD1	FD2	FD3	FD4	FD Ensemble Mean	WT − FD Ensemble Mean
					Kansas Box						
Evapotranspiration	3.356	3.292	3.016	3.012	3.169	2.672	2.576	2.692	2.732	2.668	0.501
Precipitation	3.120	2.996	3.456	3.304	3.219	3.028	2.976	2.976	3.160	3.035	0.184
Moisture convergence	−0.284	−0.440	−0.304	−0.344	−0.343	−0.088	−0.324	−0.232	−0.168	−0.203	−0.140
Change in precipitable water	0.252	0.244	0.232	0.204	0.233	0.260	0.240	0.208	0.224	0.233	0.000
Residual	−0.300	−0.388	−0.976	−0.840	−0.626	−0.704	−0.964	−0.724	−0.820	−0.803	0.177
					Indiana Box						
Evapotranspiration	4.244	3.788	4.264	4.228	4.131	4.128	4.160	4.148	4.156	4.148	−0.017
Precipitation	3.812	3.716	3.392	3.544	3.616	3.600	3.620	3.552	3.768	3.635	−0.019
Moisture convergence	−0.176	−0.436	−0.296	−0.412	−0.330	−0.432	−0.388	−0.208	−0.168	−0.299	−0.031
Change in precipitable water	−0.348	−0.372	−0.268	−0.316	−0.326	−0.332	−0.308	−0.328	−0.328	−0.324	−0.002
Residual	0.604	0.008	0.844	0.588	0.511	0.428	0.460	0.716	0.548	0.538	−0.027

[a]Units are mm/d.

around 1 August and lasting for most of the rest of the analysis period. Similar to the AZ case, though, this period of convection is initiated by a pulse of positive MC and then sustained by ET as MC becomes relatively small. Also similar, some of the extra water entering the atmosphere because of ET is transported away in a pulse of divergence at the end of the rainy period. The role of the water table, as reflected in the differences between the WT and FD ensembles (Figure 10b and Tables 1a–1b), is not as clearly delineated, but still appears to be significant. During the main wet period covering 4–19 August, both the WT-minus-FD ET and precipitation differences are usually positive, with the notable exception of some extra rain in the FD ensemble during 8–9 August. The difference in MC fluctuates significantly, and in absolute magnitude it is not always small compared to the ET and precipitation differences. However, averaged over the analysis period, both ET and precipitation are larger in the WT ensemble, and these differences are still large compared to the average difference in MC (though not as much larger as for AZ).

[32] In the KS box (Figures 9e and 9f), there is a significant transition around 11 August, from a relatively settled period characterized by relatively smaller MC (though divergence on average), small and sporadic rain events, and sustained moderate ET, to a disturbed period characterized by large values of and fluctuations in MC, heavy rain, and more variable ET with higher peak values. During the settled period, there clearly is a systematic difference between the WT and FD ensembles (Figure 10c) that is consistent with the basic AZ pattern, i.e., more ET and more precipitation in the WT simulations, and a relatively smaller difference in MC. Furthermore, the MC difference is in the wrong direction (greater divergence in the WT ensemble) to explain the enhancement of precipitation. By contrast, in the disturbed period, the MC differences between the WT and FD ensemble are much larger than the ET differences (nearly nonexistent), and there are large differences in precipitation of both positive and negative sign. Distinct from the AZ and TX cases, the average ET difference over the month between the WT and FD ensembles is significantly larger than the precipitation difference, requiring extra divergence in the WT ensemble to satisfy atmospheric water balance.

[33] From the TX and KS results, therefore, we can conclude that, during certain portions of the month, the presence of the water table is playing a similar role in enhancing ET and convective precipitation there as in AZ, though this interplay of local pathways is obscured at other times by the large-scale circulation. The results for the IN box represent the endpoint of this progression from arid to humid: precipitation events largely only occur in the presence of significant positive MC, relatively little fluctuation in ET throughout the month, and no systematic difference between the WT and FD ensembles for any of the variables (either episodically, as shown in Figure 10d, or averaged over the analysis period, as shown in Tables 1a–1b).

[34] A remaining question is the following: To what extent is the presence of the water table throughout the model domain responsible for differences in large-scale moisture convergence between the two ensembles? In other words, if there is more water table–induced ET upwind of a given region, will that lead to more net moisture flux into the region, and hence possibly more precipitation? A comprehensive answer to this question probably requires Lagrangian tracking of individual air parcels, and as such is beyond the scope of this paper. Across the four boxes, we see both positive and negative differences in MC, both at the event scale and in longer-term averages. This suggests that either this "nonlocal" water table effect is not particularly important, or that its strength varies from region to region, or that any such effect is generally difficult to distinguish from random internal dynamical variability between the ensembles.

5. Summary and Conclusions

[35] In this study, we carry out fully coupled land-atmosphere simulations with RAMS-Hydro to investigate the role of water table dynamics in controlling soil moisture, ET, boundary layer dynamics, and precipitation. Specifically, we create two ensembles of four simulations each over North America for the 1997 warm season: one, WT, with full horizontal and vertical water table dynamics, and the other, FD, with simple, free, gravity drainage of soil water.

[36] We show that this water table–induced wetter soil in the WT ensemble indeed tends to lead to enhanced ET in the more arid western regions where soil water is a strong limiting factor of ET. However, in the more humid eastern regions, where ET is limited more by surface energy availability, the wetter soil in the WT does not generally lead to systematic increases in ET over the FD ensemble.

[37] The enhanced ET due to the presence of the water table in these more arid regions also tends to lead to increased precipitation. During the warm season, much of the U.S. is in a convection-dominated precipitation regime, and when and how much rain falls is largely governed by the sometimes complex interplay between large-scale moisture convergence and local land-atmosphere interactions. We examined time series of various land and atmospheric quantities, as well as the key terms in the atmospheric water budget, to better understand the role of the water table in this interplay. We found that, in more arid regions, large-scale moisture convergence periodically initiates convection following dry periods, and then ET sustains precipitation for the duration of the subsequent wet period via recycling. In these regions, the presence of the water table in the model significantly enhances both ET and precipitation, through slower drainage and the availability of water table–fed soil moisture. Transitioning toward the more humid regions of the east, both the progressively lesser role of the water table in controlling ET, and the progressively greater role of large-scale moisture convergence compared to ET in controlling precipitation, combine to eventually eliminate the water table as a factor in precipitation.

[38] Therefore, the hypotheses posed in the Introduction appear to be valid. However, we caution that these results are based on a set of simulations of only 6 months of a single year. Simulations of other years, in particular including hydroclimatic extremes, would help demonstrate the robustness of these conclusions over a wider spectrum of variability.

[39] Interpreting our results within the *Koster et al.* [2004] "hot spot" concept, i.e., that land-atmosphere coupling strength is strongest in certain locations within the

arid-to-wet transition zone, we suggest that the inclusion of the water table in climate model simulations reveals another potential "hot spot," namely, climatologically arid regions with large topographic relief. This is because the lateral groundwater convergence in steep terrain concentrates what little precipitation there is into small regions (valleys), allowing even an arid climate to host a shallow water table, and therefore high enough soil moisture concentrations to influence precipitation.

[40] All of these results suggest that, while including an explicit water table in a climate model does not always make a large difference in the atmospheric simulation, sometimes it does. Furthermore, RAMS-Hydro, by explicitly coupling variations in the water table, streamflow, and climate, is a tool for investigating changes in water resources as a result of both changing climate and anthropogenic modifications of the hydrologic cycle, such as dam operation, groundwater pumping, and irrigation. Therefore, this study supports the use of explicit calculations of water table dynamics in comprehensive climate model studies.

[41] **Acknowledgments.** This research is supported by NSF grant ATM-0450334. G. M.-M. is supported by the Ramón y Cajal program of the Spanish Ministry of Education and Science. C. P. W. states that the views expressed in this paper are his own and those of the other authors and do not necessarily reflect the views or policies of the U.S. Environmental Protection Agency.

References

Arakawa, A., and R. V. Lamb (1977), Computational design of the basic dynamical processes of the UCLA general circulation model, *Methods Comput. Phys.*, *17*, 174–265.

Betts, A. (2004), Understanding hydrometeorology using global models, *Bull. Am. Meteorol. Soc.*, *85*, 1673–1688.

Brubaker, K. L., D. Entekhabi, and P. S. Eagleson (1993), Estimation of continental precipitation recycling, *J. Clim.*, *6*, 1077–1089.

Dirmeyer, P. A. (2006), The hydrologic feedback pathway for the land-climate coupling, *J. Hydrometeorol.*, *7*, 857–867.

Entekhabi, D., I. Rodriguez-Itube, and F. Castelli (1996), Mutual interaction of soil moisture state and atmospheric processes, *J. Hydrol.*, *184*, 3–17.

Fan, Y., G. Miguez-Macho, C. P. Weaver, R. Walko, and A. Robock (2007), Incorporating water table dynamics in climate modeling: 1. Water table observations and the equilibrium water table, *J. Geophys. Res.*, *112*, D10125, doi:10.1029/2006JD008111.

Findell, K. L., and E. A. B. Eltahir (2003a), Atmospheric controls on soil moisture-boundary layer interactions; Part I: Framework development, *J. Hydrometeorol.*, *4*, 552–569.

Findell, K. L., and E. A. B. Eltahir (2003b), Atmospheric controls on soil moisture-boundary layer interactions; part II: Feedbacks within the continental United States, *J. Hydrometeorol.*, *4*, 570–583.

Findell, K. L., and E. A. B. Eltahir (2003c), Atmospheric controls on soil moisture-boundary layer interactions: Three-dimensional wind effects, *J. Geophys. Res.*, *108*(D8), 8385, doi:10.1029/2001JD001515.

Georgescu, M., C. P. Weaver, R. Avissar, R. L. Walko, and G. Miguez-Macho (2003), Sensitivity of model-simulated summertime precipitation over the Mississippi River Basin to the spatial distribution of initial soil moisture, *J. Geophys. Res.*, *108*(D22), 8855, doi:10.1029/2002JD003107.

Harrington, J. Y. (1997), The effects of radiative and microphysical processes on simulated warm and transition season Arctic stratus, *Atmos. Sci. Pap. 637*, 289 pp., Dep. of Atmos. Sci., Colo. State Univ., Fort Collins, Colo.

Hoffman, R. N., and E. Kalnay (1983), Lagged average forecasting, an alternative to Monte Carlo forecasting, *Tellus, Ser. A*, *35*, 100–118.

Kain, J. S., and J. M. Fritsch (1993), Convective parameterization for mesoscale models: The Kain-Fritsch Scheme, in *The Representation of Cumulus Convection in Numerical Models*, *Meteorol. Monogr.*, *24*, 165–170.

Kanamitsu, M., and K. C. Mo (2003), Dynamical effect of land surface processes on summer precipitation over the southern United States, *J. Clim.*, *16*, 496–509.

Kanamitsu, M., W. Ebisuzaki, J. Woollen, S.-K. Yang, J. J. Hnilo, M. Florino, and G. L. Potter (2002), NCEP-DOE AMIP-II reanalysis (R-2), *Bull. Am. Meteorol. Soc.*, *83*, 1631–1643.

Koster, R. D., et al. (2004), Regions of strong coupling between soil moisture and precipitation, *Science*, *305*, 1138–1140.

Mellor, G. L., and T. Yamada (1982), Development of a turbulence closure model for geophysical fluid problems, *Rev. Geophys.*, *20*, 851–875.

Miguez-Macho, G., G. Stenchikov, and A. Robock (2004), Spectral nudging to eliminate the effects of domain position and geometry in regional climate model simulations, *J. Geophys. Res.*, *109*, D13104, doi:10.1029/2003JD004495.

Miguez-Macho, G., G. Stenchikov, and A. Robock (2005), Regional climate simulations over North America: Interaction of local processes with improved large-scale flow, *J. Clim.*, *18*, 1227–1246.

Miguez-Macho, G., Y. Fan, C. P. Weaver, R. Walko, and A. Robock (2007), Incorporating water table dynamics in climate modeling: 2. Formulation, validation, and soil moisture simulation, *J. Geophys. Res.*, *112*, D13108, doi:10.1029/2006JD008112.

Montaldo, N., and J. D. Albertson (2003), Temporal dynamics of soil moisture variability: 2. Implications for land surface models, *Water Resour. Res.*, *39*(10), 1275, doi:10.1029/2002WR001618.

Pal, J. S., and E. A. B. Eltahir (2002), Teleconnections of soil moisture and rainfall during the 1993 midwest summer flood, *Geophys. Res. Lett.*, *29*(18), 1865, doi:10.1029/2002GL014815.

Pielke, R. A., Sr. (2001), Influence of the spatial distribution of vegetation and soils on the prediction of cumulus convective rainfall, *Rev. Geophys.*, *39*, 151–177.

Reynolds, R. W., N. A. Rayner, T. M. Smith, D. C. Stokes, and W. Wang (2002), An improved in situ and satellite SST analysis for climate, *J. Clim.*, *15*, 1609–1625.

Sarith, P. P. M., and R. D. Koster (2005), AGCM biases in evapotranspiration regime: Impacts on soil moisture memory and land-atmosphere feedback, *J. Hydrometeorol.*, *6*, 656–669.

Schubert, S. D., M. J. Suarez, P. J. Pegion, R. D. Koster, and J. T. Bacmeister (2004), Causes of long term drought in the U.S. Great Plains, *J. Clim.*, *17*, 485–503.

Small, E. E. (2001), The influence of soil moisture anomalies on variability of the North American Monsoon system, *Geophys. Res. Lett.*, *28*, 139–142.

Timbal, B., S. Power, R. Colman, J. Viviand, and S. Lirola (2002), Does soil moisture influence climate variability and predictability over Australia?, *J. Clim.*, *15*, 1230–1238.

Walko, R. L., and C. J. Tremback (2000), Regional Atmospheric Modeling System user's guide: Version 4.2MRC, ASTeR internal report, ASTeR Div., Mission Res. Corp., Fort Collins, Colo.

R. O. Anyah and A. Robock, Department of Environmental Sciences, Rutgers University, 14 College Farm Road, New Brunswick, NJ 08901, USA. (anyah@cep.rutgers.edu; robock@envsci.rutgers.edu)

Y. Fan, Department of Earth and Planetary Sciences, Rutgers University, 610 Taylor Road, Wright Labs, Piscataway, NJ 08854, USA. (yingfan@rci.rutgers.edu)

G. Miguez-Macho, Nonlinear Physics Group, Universidade de Santiago de Compostela, E-15706 Santiago de Compostela, Spain. (gonzalo@envsci.rutgers.edu)

C. P. Weaver, Global Change Research Program, U.S. Environmental Protection Agency (8601-P), 1200 Pennsylvania Avenue, Washington, DC 20460, USA. (weaver@envsci.rutgers.edu)